Journal of Neurochemistry, 2004, **91**, 1138–1150 doi:10.1111/j.1471-4159.2004.02801.x

Functional characterization of mouse α4β2 nicotinic acetylcholine receptors stably expressed in HEK293T cells

Mark S. Karadsheh,* M. Salman Shah,* Xin Tang,† Robert L. Macdonald† and Jerry A. Stitzel‡

*Department of Pharmacology, University of Michigan Medical School, Ann Arbor, Michigan, USA

†Department of Neurology, Vanderbilt University Medical School, Nashville, Tennessee, USA

‡Department of Integrative Physiology and Institute for Behavioral Genetics, University of Colorado, Boulder, Colorado, USA

Abstract

Mouse α4β2 nicotinic acetylcholine receptors (nAchRs) were stably expressed in HEK293T cells. The function of this stable cell line, termed mmα4β2, was assessed using an aequorin-based luminescence method that measures agonist-evoked changes in intracellular calcium. Agonist-elicited changes in intracellular calcium were due primarily to direct entry of calcium through the α4β2 channel, although release of calcium from intracellular stores contributed ~ 28% of the agonist-evoked response. Agonist pharmacologies were very similar between the mmα4β2 cells and most cell lines that stably express human α4β2 nAchRs. Based on agonist profiles and sensitivity to the antagonist dihydro-β-erythroidine (DHβE), the predominant α4β2 nAchR expressed in the mmα4β2 cells exhibits a pharmacology that most resembles the DHβE-sensitive component of $^{86}Rb^{+}$ efflux from mouse brain synaptosomes. However, when evaluated with the aequorin assay, the mmα4β2 nAchR was found to be atypically sensitive to blockade by the presumed α7-selective antagonist methyllycaconitine (MLA), exhibiting an IC_{50} value of 31 ± 0.1 nM. Similar IC_{50} values have been reported for the MLA inhibition of nicotine-stimulated dopamine release, a response that is mediated by β2-subunit-containing nAchRs and not α7-subunit-containing nAchRs. Consequently, at low nanomolar concentrations, MLA may not be as selective for α7-containing nAchRs as previously thought.

Keywords: aequorin, calcium, heterologous expression, luminescence, methyllycaconitine.

J. Neurochem. (2004) **91,** 1138–1150.

Alterations in intracellular calcium levels in neurons can affect a wide range of cellular processes including changes in gene expression, synaptic plasticity, neurotransmission and neurotransmitter release (for review, see Berridge 1998). Changes in intracellular calcium levels in neurons and glia can arise from the entry of calcium via ligand- and voltage-gated ion channels, as well as from the release of calcium from distinct intracellular stores. Neuronal nicotinic acetylcholine receptors (nAchRs), like ionotropic glutamate receptors, are ligand-gated ion channels that exhibit high permeability to calcium (Vernino *et al*. 1992; Bertrand *et al*. 1993; Seguela *et al*. 1993; Role and Berg 1996; Ragozzino *et al*. 1998). Assembled from distinct combinations of subunits of the neuronal nAchR subunit family, numerous nAchR subtypes are expressed in the brain (Lindstrom 2003). The neuronal nAchR subunit family includes nine α subunits, designated α2–α10 and three β subunits designated β2– β4. The nAchR subtype that exhibits the greatest calcium permeability relative to sodium is the α7 homomeric nAchR (Bertrand *et al*. 1993; Seguela *et al*. 1993; Castro and Albuquerque 1995). Another nAchR subtype that is calcium permeable is the subtype composed of α4 and β2 subunits (Vernino *et al*. 1992; Ragozzino *et al*. 1998).

The α4β2 nAchR is the most abundant nAchR subtype expressed in the brain, and studies have demonstrated that this receptor subtype is located presynaptically on

Received April 28, 2004; revised manuscript received July 22, 2004; accepted July 28, 2004.

Address correspondence and reprint requests to Jerry Stitzel, Ph.D., Institute for Behavioral Genetics, University of Colorado, UCB 447, Boulder, CO 80309–0447, USA. E-mail: Stitzel@colorado.edu

Abbreviations used: A85380, 3-(2-(*S*)-azetidinylmethoxy) pyridine dihydrochloride; Ach, acetylcholine; DEC, decamethonium; DHβE, dihydro-β-erythroidine; DMEM, Dulbecco's modified Eagle's medium; DMPP, dimethylphenylpiperazinium iodide; HEX, hexamethonium; MCC, methylcarbamylcholine chloride; MEC, mecamylamine; MLA, methyllycaconitine; nAchR, nicotinic acetylcholine receptor; PBS, phosphate-buffered saline; TMA, tetramethylammonium chloride.

GABAergic (Alkondon *et al*. 1996; Lu *et al*. 1998; Zhu and Chiappinelli 1999; Klink *et al*. 2001) and dopaminergic terminals (Grady *et al*. 1992; Klink *et al*. 2001; Champtiaux *et al*. 2002; Zoli *et al*. 2002). This nAchR subtype is elevated in brain tissue from smokers (Benwell *et al*. 1988; Breese *et al*. 1997) and reduced in brain tissue from Alzheimer's disease patients (Flynn and Mash 1986; Nordberg and Winblad 1986; Whitehouse *et al*. 1986). Rare alleles for the genes that encode the α4 and β2 subunits have been identified in humans and are associated with autosomal-dominant nocturnal frontal lobe epilepsy (Steinlein 2004 for review).

Like humans, mice chronically exposed to nicotine exhibit an increase in α4β2 nAchRs in brain (Marks *et al*. 1983). In addition, mice engineered to lack this nAchR subtype exhibit learning deficits (Picciotto *et al*. 1995), loss of the neuroprotective effect of nicotine on 6-OH DOPA lesions in the striatum (Ryan *et al*. 2001) and do not show reinforcement by nicotine (Epping-Jordan *et al*. 1999). Studies have also described a polymorphism in the mouse α4 subunit gene that is associated with functional differences in α4β2 nAchRs in mouse brain synaptosomes (Stitzel *et al*. 2001; Dobelis *et al*. 2002) and affects receptor function in a heterologous expression system (Kim *et al*. 2003). This polymorphism is associated with mouse strain differences in sensitivity to nicotine-induced seizures (Stitzel *et al*. 2000) and other responses to nicotine (Tritto *et al*. 2002; Butt *et al*. submitted), as well as individual differences in responsiveness to alcohol (Owens *et al*. 2003; Butt *et al*. 2004).

Owing to the heterogeneity of nAchRs in the brain, it is difficult to evaluate the pharmacology and cell biology of individual native nAchR subtypes. This complication limits the ability to assess how variations in receptor function of specific nAchR subtypes might contribute to such processes as addiction and disease. In an attempt to establish the pharmacology and cell biology of individual nAchR subtypes, several heterologous expression systems that stably express specific nAchR subtypes, including the α4β2 nAchR subtype (Gopalakrishnan *et al*. 1996; Chavez-Noriega *et al*. 2000; Michelmore *et al*. 2002; Eaton *et al*. 2003; Nelson *et al*. 2003) have been developed. However, despite the increasing number of these nAchR-expressing cell lines, an extensive comparison of the pharmacology of receptor function between these cell lines and native α4β2 nAchRs has not been reported. In the data described here, HEK293T cells that exhibit stable expression of a functional mouse α4β2 nAchR are described. Agonist-evoked increases in intracellular calcium by eight agonists and inhibition of the agonist-evoked response by five antagonists were assessed in this cell line. In addition, the mechanism of agonist-induced changes in intracellular calcium in this cell line was evaluated. Finally, in order to evaluate the similarity between heterologously expressed mouse α4β2 nAchRs and native mouse α4β2 nAchRs, the agonist and antagonist profiles of the mouse α4β2 cell line were compared with the pharmacological profiles of native α4β2 nAchR-mediated $^{86}Rb^{+}$ efflux from mouse brain thalamic synaptosomes.

Materials and methods

Cell culture

HEK293T cells were maintained at 37°C in a humidified, 5% CO_2 environment in Dulbecco's modified Eagle's medium (high glucose, no pyruvate) (DMEM), 10% heat-inactivated fetal bovine serum and antibiotic/antimycotic (100 U/mL penicillin, 100 μg/mL streptomycin and 0.25 μg/mL amphotericin B). Culture reagents were purchased from either Biowhittaker (East Rutherford, NJ, USA) or Invitrogen (Carlsbad, CA, USA).

Generation of a HEK293T cell line stably transfected with mouse α4 and β2 nAchR subunits

Mouse nAchR α4 and β2 subunit cDNAs were introduced into the mammalian expression vectors pcDNA3.1zeo (Invitrogen) and pcDNA3.1hygro (Invitrogen), respectively, as previously described (Kim *et al*. 2003). For transfection, HEK293T cells were plated at a density of 5×10^6 cells/100 mm dish in DMEM supplemented with 10% fetal bovine serum and antibiotic/antimycotic. The day following plating, the cells were transfected with the mouse α4 and β2 cDNA constructs using LipoFectamine Plus Reagent (Invitrogen) according to the manufacturer's suggested protocol. The A529 variant of the mouse α4 cDNA (Kim *et al*. 2003) was used for the transfection. Approximately 48 h following transfection, the media was supplemented with 0.05 mg/mL zeocin (Invitrogen) and 0.25 mg/mL hygromycin sulfate in order to select for cells that had stably integrated the α4 and β2 expression vectors, respectively. Following 1 week of selection with zeocin and hygromycin, the concentrations of these drugs were increased to 0.1 and 0.5 mg/mL, respectively. The cells then were maintained under these conditions for 2–3 additional weeks. After this drug selection period, the cells were trypsinized and transferred to a new culture vessel. The cells always were maintained under selection with 0.1 mg/mL zeocin and 0.5 mg/mL hygromycin.

Isolation of stable transfectants enriched for surface nAchR expression

Pooled, stably transfected cells were removed from a near confluent 75 cm^2 flask by gentle aspiration with phosphate-buffered saline (PBS) and transferred to a 5 mL sterile polypropylene tube. Following centrifugation at 4°C for 5 min at 800 *g*, the PBS was removed and the cells were resuspended at a density of 5×10^6 cells/mL in PBS supplemented with 2% heat-inactivated fetal bovine serum and 0.05% sodium azide (flow buffer). The antiα4-specific monoclonal antibody mAb299 (Covance, Berkeley, CA, USA) (Whiting and Lindstrom 1988) was added to the cells at a 1/500 dilution and the cells were incubated for 1 h at 4°C with gentle rocking. After incubation with mAb299, the cells were centrifuged as described above, rinsed with flow buffer, and centrifuged once again as described above. The wash and centrifugation steps were repeated a total of three times. After the third wash, the cells were resuspended in flow buffer and a

biotin-conjugated rabbit antirat polyclonal antibody (Zymed Laboratories, South San Francisco, CA, USA) was added to the cell suspension at a 1/500 dilution. The cells then were incubated at 4°C for 30 min with gentle rocking and subsequently washed exactly as described above. Upon completion of the wash steps, the cells were resuspended in flow buffer, streptavidin-conjugated phycoerythrin was added to the cell suspension at a 1/200 dilution, and the cells were incubated at 4°C in the dark for 20 min with gentle rocking. Following this incubation, cells were centrifuged as described above, resuspended in PBS + 0.05% sodium azide and recentrifuged. Resuspension of the cells and centrifugation was repeated a total of three times. After the final wash and centrifugation step, the cells were resuspended at a density of 5×10^6 cells/mL in PBS + 0.05% sodium azide. Propidium iodide was added to the cells at a final concentration of 2.5 μg/mL and following 5 min incubation, the cells were transported to the University of Michigan Flow Cytometry Core. Viable cells that were surface-positive for mAb299 were sterile sorted by the Flow Cytometry Core. To identify viable, mAb299 surface-positive cells, the stable transfectants were compared against non-transfected HEK293T cells that had been mAb299 stained side-by-side with the stable line. Approximately 37% of the cells analyzed were identified as viable, mAb299-positive cells.

The mAb299-positive cells were seeded in a culture flask in DMEM, 10% fetal bovine serum, antibiotic/antimycotic solution and selection drugs as described above and allowed to propagate to near confluence. Subsequent passages (passages 1–10) of these cells were used for all experiments in this report. These cells were designated as mmα4b2 (*Mus musculus* α4β2).

[^{3}H]-epibatidine binding

mmα4β2 cells were seeded at a density of 5×10^6 cells/100 mm dish. Approximately 72 h after plating, the cells were scraped from the dishes and membrane fractions were prepared as previously described (Marks *et al*. 1998), with the exception that a 15 min incubation at 37°C with 50 μg/mL DNAse was performed prior to the first centrifugation. The binding of [^{3}H]-epibatidine to the membrane fractions was performed in a 250 μL reaction that included KRH buffer (118 mM NaCl, 4.8 mM KCl, 2.5 mM $CaCl_2$, 1.2 mM Mg_2SO_4 and 20 mM HEPES pH 7.5) and varying concentrations of [^{3}H]-epibatidine. Non-specific binding was determined by the inclusion of 10 μM nicotine in the reaction. The binding reaction was terminated by filtration of the protein onto glass fiber filters that had been treated with 0.5% polyethylenimine in KRH buffer. Filtration was performed using a Tomtec Mach II cell harvester (Tomtec, Hamden, CT, USA). After filtration, the filters were washed four times with ice-cold buffer. The filters were collected and placed in scintillation vials. Following the addition of 3 mL scintillation fluid, the radioactivity was measured using a liquid scintillation counter (Beckman Coulter, Fullerton, CA, USA). Preliminary experiments were performed to determine the amount of cell membrane homogenate that would provide detectable binding without ligand depletion at low ligand concentrations. Ligand depletion was defined as c.p.m. of membrane-bound [^{3}H]-epibatidine/c.p.m. of total [^{3}H]-epibatidine $>25\%$. Subsequent ligand binding was performed with an amount of homogenate that did not produce ligand depletion. Homogenate protein levels were determined by the method of Lowry (Lowry *et al*. 1951).

Electrophysiological recording from mmα4β2 cells

mmα4β2 cells were maintained in a humidified 5% CO_2 environment at 37°C in DMEM supplemented with 10% fetal bovine serum and antibiotics (100 U/mL penicillin, 100 μg/mL streptomycin). Between 24 and 48 h prior to recording, the cells were plated at a density of 3×10^5 cells/60 mm dish and maintained in a humidified 5% CO_2 environment at 30°C. For whole-cell recording, the external solution consisted of 140 mM NaCl, 5 mM KCl, 1 mM $MgCl_2$, 2 mM $CaCl_2$, 10 mM glucose, 10 mM HEPES, pH 7.3. Recording electrodes were filled with an internal solution of 140 mM CsCl, 4 mM NaCl, 4 mM $MgCl_2$, 0.5 mM $CaCl_2$, 5 mM EGTA, 10 mM HEPES pH 7.3, with 4 mM ATP added on the day of recording. nAchR receptor currents were recorded using a lifted whole-cell patch-clamp technique. Agonist was applied to cells using a modified SF-77B Perfusion Fast-Step application system (Warner Instrument Corp., Hamden, CT, USA). The application system provided for simultaneous flow of all solutions to which the cells were exposed through three parallel glass square barrels. All step protocols began with a cell positioned in the flow of external bath solution from which the multibarrelled array was repositioned such that the unmoved cell and electrode were now exposed to acetylcholine (Ach). All cells were voltage clamped at −50 mV during recordings. Currents were recorded using a 200B amplifier (Axon Instruments, Union City, CA, USA). All experiments were performed at room temperature (22°C). Whole cell currents were analyzed using the programs PCLAMP 9.0 and PRISM (GraphPad, San Diego, CA). Whole-cell current amplitudes were obtained by measuring the peak current evoked during the application of drug. For Ach and tetramethylammonium chloride (TMA) concentration–response curves, the data were normalized to a percent of the maximum current elicited by saturating agonist concentrations for each cell. For methyllycaconitine (MLA) inhibition curves, MLA was applied to the cells for 1 s prior to the application of a solution containing 10 μM nicotine and the pre-application concentration of MLA. Normalized concentrationresponse data were curve fitted using the sum of two Michaelis–Menten equations.

Aequorin intracellular calcium measurement assay

Cell preparation

mmα4β2 cells were seeded onto six-well plates (1×10^6 cells/well) or 100 mm dishes (5×10^6 cells/dish) and the following day transfected with the plasmid pcDNA into which a human codon-optimized aequorin cDNA had been cloned (Vernon and Printen 2002). Transfection was performed using the LipofectAmine Plus Reagent as recommended by the manufacturer (Invitrogen). Approximately 48–72 h following transfection, culture media was replaced with DMEM + 0.1% fetal bovine serum and 2.5 μM coelenterizine-hcp (Molecular Probes, Eugene, OR, USA) and the cells were incubated for 3–4 h at 37°C in a humidified 5% CO_2 incubator. Following the coelenterizine incubation, cells were gently aspirated from the culture dishes and transferred to either 2 mL (six-well plates) or 15 mL (100 mm dishes) centrifuge tubes. An equal volume of Hank's balanced salt solution supplemented with 100 mM calcium chloride was added and the cells were incubated for 5–10 min at room temperature. This step eliminated an artifactual injection peak presumably resulting from entry of calcium into non-viable permeable cells. The cells were then pelleted by centrifugation at 4°C for 5 min at 800 *g*, the supernatant was

discarded, and the cells were resuspended in 1× assay buffer (130 mM NaCl, 5.4 mM KCl, 10 mM $CaCl_2$, 5 mM glucose, 25 mM HEPES, pH 7.5) and again pelleted by centrifugation. Subsequently, the cells were resuspended in fresh 1× assay buffer (1 mL/well of a six-well plate or 6 mL/100 mm dish) and incubated for 1–2 h at 4°C prior to initiating the assay.

Aequorin assay

For agonist concentration–response curves, 50 μL of each agonist concentration (in assay buffer) was added to each well of a 96-well opaque plate which was placed in a Beckman-Coulter LD400 luminometer. mmα4β2 cells were placed in a 7 mL scintillation vial connected to a luminometer injector line and gently mixed continuously with a stir bar. For Ach stimulations, the cells were incubated with 1 μM atropine for 10–15 min at room temperature prior to initiating the assay. The assay was initiated by injection of 50 μL of cells into each well of the agonist-containing plate. Agonist-stimulated luminescence was recorded at 0.15–0.2 s intervals for 15–20 s immediately following the addition of cells to each well. Each agonist concentration was measured in duplicate per aequorin transfection. Once the concentration–response recordings were complete for an entire 96-well plate, remaining aequorin luminescence was determined by injecting 100 μL of a solution containing 0.1% Triton X-100 and 100 mM $CaCl_2$ into each well and recording luminescence for 5 s at 0.1 s intervals. In order to control for differences in cell number per well and variation in the transfection efficiency of aequorin, agonist-stimulated luminescence was normalized by dividing the maximal peak value for the agonist-stimulated luminescence (L) by the total peak luminescence value (L_{max}) (maximal peak agonist-stimulated luminescence + maximal peak luminescence resulting from cell lysis in the presence of high calcium). All data, except raw data traces, are presented as the percent of total possible calcium-stimulated luminescence (L/L_{max}).

For antagonist concentration response curves, 25 μL of mmα4β2 cells was added to each well of an opaque 96-well plate along with 25 μL of the appropriate antagonist. The cells and antagonists were mixed and incubated for 10 min at room temperature. Following the 10 min incubation, 50 μL of 10 μM nicotine was injected onto the cells and luminescence was recorded at 0.2 s intervals for 20 s. Marks *et al*. (1999) used a concentration of 10 μM nicotine to evaluate antagonists IC_{50} values for a 'dihydro-β-ethroidine sensitive' α4β2 nAchR subtype present in mouse brain synaptosomes. Therefore, 10 μM nicotine was used for the antagonist experiments with the mmα4β2 cells so that a comparison of the IC_{50} values could be made between the mmα4β2cells and 'dihydro-β-ethroidine sensitive' α4β2nAchRs present in mouse brain synaptosomes. After agonist incubation, total luminescence per well was recorded by injection of 100 μL of 0.1% Triton X-100 and 100 mM $CaCl_2$ and recording luminescence for 5 s at 0.1 s intervals. All data are presented as L/L_{max} as described above.

Experiments with the voltage-sensitive calcium channel inhibitor $CdCl_2$ (100 μM), and the inhibitors of intracellular calcium release, ryanodine (30 μM) and xestospongin C (10 μM), were performed exactly as described for the antagonist experiments with the exceptions that the cells were incubated with the compounds for 30 min prior to agonist application and 1 μM epibatidine was used as the agonist rather than 10 μM nicotine. The concentration used for each inhibitor was based on data from others (Gafni *et al*. 1997; Gueorguiev *et al*. 2000; Sharma and Vijayaraghavan 2001; Shoop *et al*. 2001; Dajas-Bailador *et al*. 2002).

Data analysis

Whole cell recording data were fitted to a two-site model using the sum of two Michaelis–Menten equations. Concentration–response curves for the aequorin assay were fitted to a four parameter logistic equation using PRISM 3.0 software. All data are represented as mean ± S.E.M.

Results

Generation of a cell line that expresses mouse α4β2 nicotinic receptors

Plasmids carrying the cDNAs for the mouse nAchR subunits α4 and β2 were transfected into HEK293T cells as described above. Following several weeks of growth in media supplemented with zeocin and hygromycin to select for cells that had stably integrated both plasmids, the cells were pooled and viable cells that were surface positive for the α4 subunit were immuno-isolated with the α4 subunit-specific antibody mAb299 (Whiting and Lindstrom 1988) by fluorescence-activated cell sorting. Approximately 37% of the viable cells were selected as mAb299 immunopositive. These immunopositive cells, hereafter referred to as mmα4β2, were propagated for experimental procedures. All experiments described in this report utilized the mmα4β2 cells between generations 2 and 10.

Ligand binding of mmα4β2 cells

To verify the expression of α4β2 nAchRs in the mmα4β2 cells, saturation binding with [^{3}H]-epibatidine was performed (Fig. 1). Results of the ligand binding indicated that the cells expressed α4β2 nAchRs with a K_D value for [^{3}H]-epibatidine

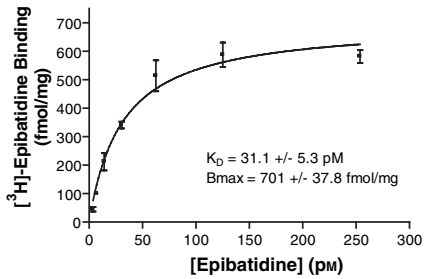

Fig. 1 Saturation binding of [^{3}H]-epibatidine to mmα4β2 cell membrane fractions. Particulate fractions prepared from mmα4β2 cells were incubated with [^{3}H]-epibatidine concentrations ranging between 3.8 and 500 pM. The binding of [^{3}H]-epibatidine to the particulate fractions was measured under conditions that minimized ligand depletion as described in Materials and methods. The K_D value for the receptors expressed in the mmα4β2 receptors was calculated to be 31.1 ± 5.3 pM. The B_{max} value for the mmα4β2 cells was 701 ± 37.8 fmol/mg protein. Data represent the mean ± SEM of three separate membrane preparations of the mmα4β2 cells.

of 31.1 ± 5.3 pM and a B_{max} of 701 ± 37.8 fmol/mg protein. The K_D value is consistent with the K_D for endogenous (Marks *et al*. 1998; Shafaee *et al*. 1999; Truong *et al*. 2001) and heterologously expressed α4β2 nAchRs (Shafaee *et al*. 1999; Chavez-Noriega *et al*. 2000; Truong *et al*. 2001; Eaton *et al*. 2003). The B_{max} value is similar to that reported for other stable cell lines expressing heterologous α4β2 nAchRs (Chavez-Noriega *et al*. 2000; Michelmore *et al*. 2002; Eaton *et al*. 2003).

mmα4β2 cells express functional α4β2 nAchRs

Whole-cell patch-clamp recording established that the mmα4β2 cells express functional α4β2 nAchRs. Figure 2 shows the concentration–response of the mmα4β2 cells to Ach. Curve fitting indicated that the Ach response curve was consistent with a two-component response with the low-affinity response exhibiting an EC_{50} of 179 ± 22 μM, and the high-affinity component possessing an EC_{50} value of 3.36 ± 2.25 μM. The low-affinity component was responsible for ˜ 90% of the total response. The high proportion of the low-affinity response relative to the high-affinity response is consistent with other reports on the stable expression of α4β2 nAchRs in HEK cells (Buisson and Bertrand 2001; Nelson *et al*. 2003).

Agonist-stimulated increase in intracellular calcium: requirement for extracellular calcium

In order to further characterize the function of the mmα4β2 cell line, agonist-stimulated changes in intracellular calcium were determined using an aequorin-based luminescence assay (Brini *et al*. 1995; Vernon and Printen 2002). Several studies have demonstrated that the measurement of nicotinic receptor-mediated changes in intracellular calcium is dependent upon the concentration of extracellular calcium (Ragozzino *et al*. 1998; Xiao *et al*. 1998; Chavez-Noriega *et al*. 2000; Pacheco *et al*. 2001; Michelmore *et al*. 2002). Therefore, the extracellular calcium requirement for nicotinic agonist-stimulated changes in intracellular calcium in the mmα4β2 cell line was addressed by stimulating aequorin-transfected mmα4β2 cells with 1 μM epibatidine in the presence of concentrations of extracellular calcium ranging from nominally 0 to 10 mM. Figure 3 shows the raw data traces of 1 μM epibatidine-stimulated luminescence over a 15 s recording period. Consistent with previous reports, increasing the concentration of extracellular calcium resulted in an increase in the response to the 1 μM epibatidine stimulation. Consequently, all experiments described below were performed in the presence of 10 mM calcium, the highest concentration of extracellular calcium tested.

Pharmacological characterization of agonist-induced increases in intracellular calcium in mmα4β2 cells

Eight nAchR agonists were tested for their potency and efficacy in stimulating an increase in intracellular calcium

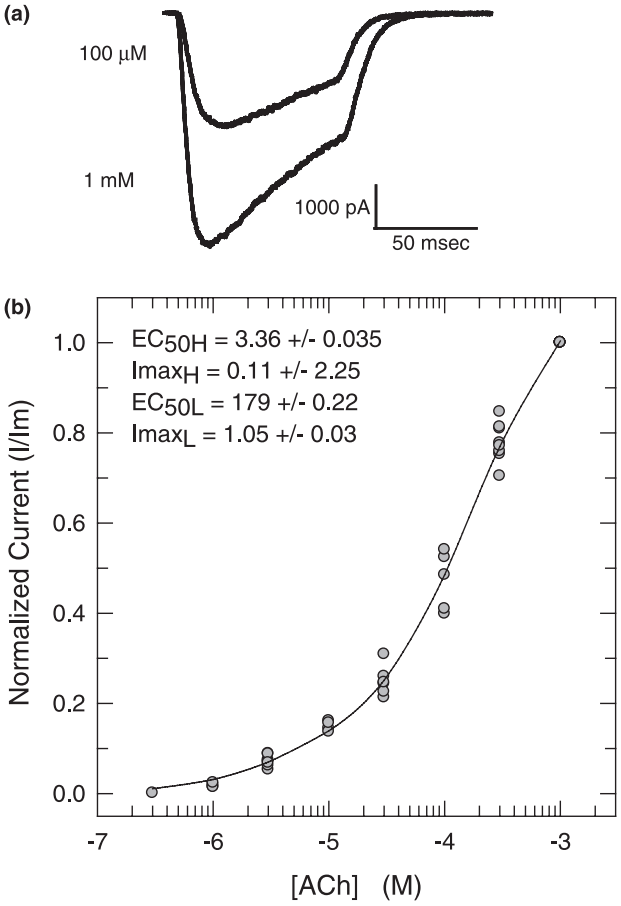

Fig. 2 Whole-cell patch-clamp Ach concentration response curve for the mmα4β2 cell line. The response of the mmα4β2 cells to Ach was measured using the lifted whole-cell patch-clamp method as described in Materials and methods. (a) Representative whole-cell currents from mmα4β2 cells. Ach was applied for 80–200 ms voltage clamped at −50 mV. (b) The concentration–response relationship was obtained by normalizing the peak response for each concentration of Ach to the maximal current response for each cell. (a) Data points for the concentration-response curve represent the mean ± SEM of between four and eight separate measurements per Ach concentration. Data were fitted using the sum of two Michaelis–Menten equations. EC_{50} values for the low- (EC_{50L}) and high-affinity (EC_{50H}) components of the Ach response curve were estimated to be 179 ± 22 and 3.36 ± 2.25 μM, respectively. Peak current for the low- (I_{maxL}) and high-affinity (I_{maxH}) components were estimated to be 1.05 ± 0.03 and 0.11 ± 0.035, respectively.

concentrations. Figure 4(a) shows the raw data traces of aequorin luminescence following stimulation with epibatidine concentrations ranging from 30 nM to 0.3 μM. As the epibatidine concentration was increased, the luminescence peak increased and became more distinct. The time to peak luminescence also decreased as the concentration of agonist increased. This concentration-dependent temporal shift in the aequorin peak response is a common feature of the aequorin-based assay. For example, Ungrin *et al*.

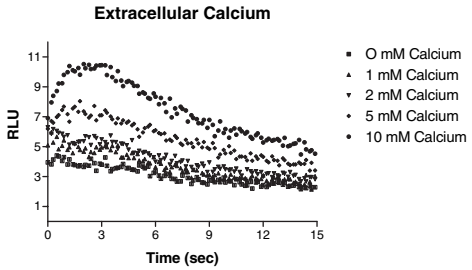

Fig. 3 Effect of extracellular calcium on epibatidine-stimulated changes in intracellular calcium in mmα4β2 cells. mmα4β2 cells were transfected with the luminescent calcium indicator protein aequorin and 48 h later loaded with the aequorin coenzyme coelenterizine-hcp as described in Materials and methods. Epibatidine (1 μM) stimulated changes in intracellular calcium in the aequorin/coelenterizine-hcp-loaded mmα4β2 cells were subsequently determined in the presence of extracellular calcium ranging from 0 (nominal) to 10 mM. Immediately following the injection of epibatidine onto the cells, luminescence (RLU = relative luminescence units) was measured at 0.15 s intervals for 15 s in a 96-well plate luminometer as described in Materials and methods. Data shown are representative traces from a single experiment.

(1999) described this temporal shift in response to increasing concentrations of prostanoids.

Concentration–response curves for epibatidine, as well as Ach, A85380, cytisine, dimethylphenylpiperazinium iodide (DMPP), methylcarbachol, nicotine and TMA are shown in Fig. 4(b). Because electrophysiological data indicated that 90% of the Ach response was due to a single component, data were fitted assuming single population kinetics. Of the agonists tested, epibatidine exhibited the lowest EC_{50} value (0.033 ± 0.001 μM) and Ach the highest (66.3 ± 2.23 μM) (Table 1). The rank order of EC_{50} values for the α4β2-mediated increase in intracellular calcium levels was epibatidine < A85380 < DMPP = nicotine < MCC < TMA < Ach. An EC_{50} value was not calculated for cytisine because the response to this drug did not fit a sigmoidal concentration–response curve. Of the agonists tested, Ach was the most efficacious in stimulating an increase in intracellular calcium, whereas cytisine was the least efficacious. The rank order of efficacy of the agonists was Ach > epibatidine = MCC = TMA > A85380 > nicotine > DMPP > cytisine (Table 1).

Antagonist inhibition of nicotine-stimulated intracellular calcium in mmα4β2 cells

The ability of the nAchR antagonists decamethonium (DEC), dihydro-β-erythroidine (DHβE), hexamethonium (HEX), mecamylamine (MEC) and MLA to inhibit the increase in intracellular calcium in response to 10 μM nicotine was assessed in the mmα4β2 cells. Raw data traces of the effect of increasing concentrations of DHβE on the nicotine-stimulated increase in intracellular calcium

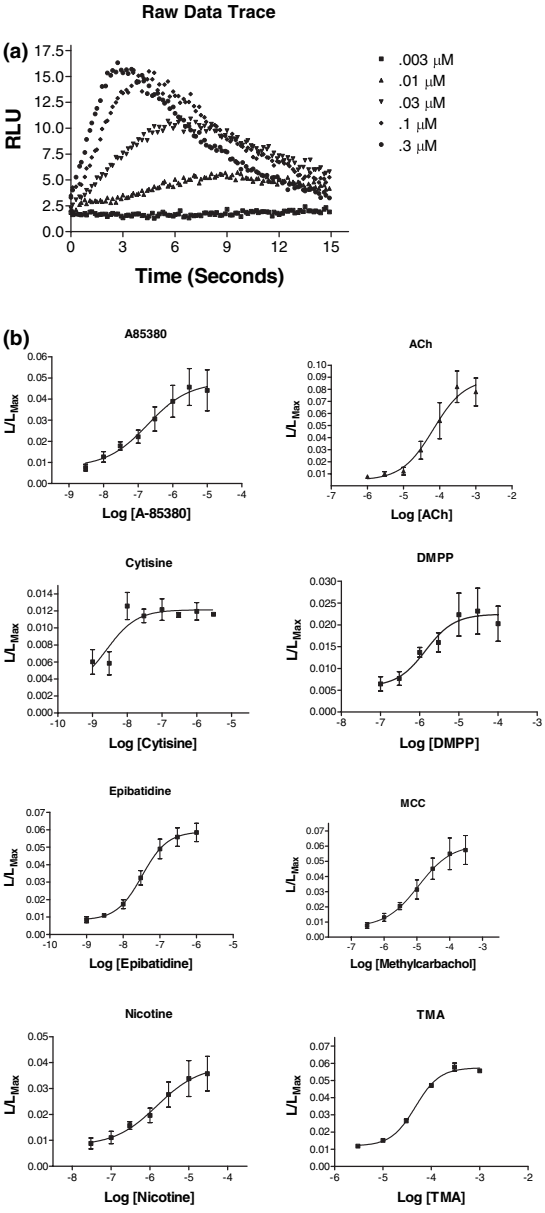

Fig. 4 Concentration–response curves for agonist induced changes in mmα4β2 cell intracellular calcium. (a) Raw data trace of concentration-dependent changes in epibatidine (3–300 nM) stimulated luminescence in aeqourin/coelenterizine-hcp-loaded mmα4β2 cells. (RLU = relative luminescence units). Immediately upon addition of epibatidine to the aeqourin/coelenterizine-hcp-loaded mmα4β2 cells, luminescence was measured at 0.15 s intervals for 15 s. (b) Concentration–response curves for agonist-induced changes in intracellular calcium. Data are represented as the ratio of agonist-induced peak aequorin luminescence (L) divided by the sum of the possible aequorin luminescence (L_{max}; peak agonist induced luminescence + peak luminescence following cell lysis in the presence of 50 mM calcium). Data shown represent mean ± SEM of between three and eight independent aequorin transfections per agonist). Data were fitted to a four-parameter logistic equation assuming a single site. EC_{50} values and maximal responses for each agonist are provided in Table 1.

Table 1 EC_{50} values (μM) and maximal responses for mmα4β2 cells

Agonist	mmα4β2 EC_{50}	R_{max}	DHβE Sensitive Marks *et al.* (1999) EC_{50}	DHβE Sensitive Marks *et al.* (1999) E_{max}	DHβE Resistant Marks *et al.* (1999) EC_{50}	DHβE Resistant Marks *et al.* (1999) E_{max}	Gopalakrishnan *et al.* (1996) EC_{50}	Chavez-Noriega *et al.* (2000) EC_{50}
A85380	0.19 ± 0.04	0.042 ± 0.004	0.018 ± 0.006	0.12 ± 0.006	40 ± 8.5	0.392 ± 0.02		
Ach	66.3 ± 2.28	0.087 ± 0.009	7.18 ± 0.29	0.149 ± 0.011	550 ± 61	0.158 ± 0.005	43.79 ± 1.18	100
Cytisine	–	0.012 ± 0.0006	0.013 ± 0.011	0.017 ± 0.003	150 ± 60	0.068 ± 0.007		
DMPP	1.43 ± 0.46	0.022 ± 0.002	6.1 ± 1.4	0.102 ± 0.005	160 ± 110	0.043 ± 0.008	2.51 ± 0.25	6.7
Epibatidine	0.033 ± 0.001	0.06 ± 0.003	0.057 ± 0.016	0.289 ± 0.019	2.2 ± 0.3	0.392 ± 0.017	0.017 ± 0.002	0.043
Methylcarbachol	11.2 ± 3.2	0.057 ± 0.005	19.4 ± 5.4	0.192 ± 0.012	730 ± 80	0.218 ± 0.007		
Nicotine	1.53 ± 0.43	0.033 ± 0.003	1.39 ± 0.42	0.112 ± 0.007	130 ± 20	0.164 ± 0.007	3.99 ± 0.11	3.5
TMA	46.9 ± 0.36	0.06 ± 0.002	185 ± 32	0.203 ± 0.009	890 ± 720	0.04 ± 0.007		

Values for the mmα4^{β2} cells were calcuted by non-linear least squares curve fitting of the data shown in Fig. 4(B) using a four-parameter logistic equation. Values given are mean ± SEM. Mean values were calculated from a minimum of three separate aequorin transfections. R_{max} = maximal response; E_{max} = maximal $^{86}Rb^{+}$ efflux.

are shown in Fig. 5(a). Full concentration–response curves for the five antagonists are provided in Fig. 5(b). MLA was the most potent antagonist at inhibiting the nicotine-stimulated increase in intracellular calcium (IC_{50} = 31.6 ± 1.2 nM), whereas HEX and DEC were the least potent (1.96 ± 0.13 and 2.52 ± 0.21 μM, respectively). The rank order of antagonist IC_{50} values was MLA < DHβE = MEC < HEX =DEC (Table 2).

Mechanism of nicotine-stimulated increase in intracellular calcium

Changes in intracellular calcium following nAchR stimulation can result from direct entry of calcium through the α4β2 nAchR, as a result of activation of voltage-sensitive calcium channels or as a consequence of the release of intracellular stores of calcium. To identify the mechanism through which α4β2 nAchR stimulation increases intracellular calcium, cells

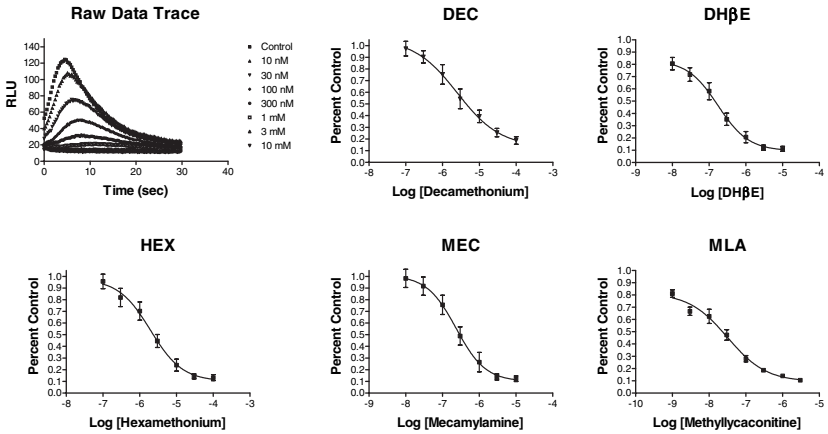

Fig. 5 Antagonist concentration–response curves for the inhibition of mmα4β2 receptor function. The ability of the nicotinic antagonists DEC, DHβE, HEX, MEC and MLA to inhibit nicotine (10 μM) stimulated luminescence in aeqourin/coelenterizine-hcp-loaded mmα4β2 cells was evaluated. The upper left-hand panel shows a raw data trace of the concentration-dependent inhibition of nicotine-stimulated aequorin luminescence by DHβE (RLU = relative luminescence units) over a 30 s recording period. mmα4β2 cells were incubated with each antagonist for 10–15 min prior to stimulation with 10 μM nicotine. Immediately upon the addition of nicotine, luminescence was recorded at 0.2 s intervals for 20 s. Data were calculated as the ratio of agonist induced peak aequorin luminescence (*L*) divided by the sum of the possible aequorin luminescence (L_{max}; peak agonist induced luminescence + peak luminescence following cell lysis in the presence of 50 mM calcium). Results presented represent the percent L/L_{max} relative to 10 μM nicotine stimulation in the absence of antagonist. Data shown represent the mean ± SEM of between three and four independent aequorin transfections per antagonist). Data were fitted to a four-parameter logistic equation. IC_{50} values for each antagonist are provided in Table 2.

Table 2 IC_{50} values (μM) for mmα4β2 cells

Antagonist	mmα4β2	Marks *et al.* (1999) DHβE Sensitive
Decamethonium	2.52 ± 0.21	4.1 ± 1.7
DHβE	0.17 ± 0.03	0.15 ± 0.05
Hexamethonium	1.96 ± 0.13	16.6 ± 6.1
Mecamylamine	0.24 ± 0.013	0.59 ± 0.09
MLA	0.03 ± 0.0012	0.20 ± 0.06

IC_{50} values were calculated using by non-linear least squares curve fitting of the curves shown in Fig. 5. Values given are mean ± SEM. Mean values were calculated from a minimum of four separate aequorin transfections.

were stimulated with 1 μM epibatidine in the presence of either 100 μM $CdCl_2$, 30 μM ryanodine or 10 μM xestospongin C as described above (Fig. 6). Inclusion of the general high-voltage sensitive calcium channel inhibitor $CdCl_2$ had no effect on the levels of epibatidine-stimulated intracellular calcium. In contrast, inhibition of ryanodine receptor-dependent intracellular calcium release by ryanodine or IP3-receptor-dependent intracellular calcium release by xestospongin C reduced epibatidine-stimulated intracellular calcium to 80 ± 1.3 and 85.4 ± 3.0% of control, respectively. Inclusion of both ryanodine and xestospongin C led to a response that was 72.1 ± 4.6% of the control response. Therefore, the nicotinic agonist-stimulated changes in intracellular calcium as measured with the aequorin-based assay

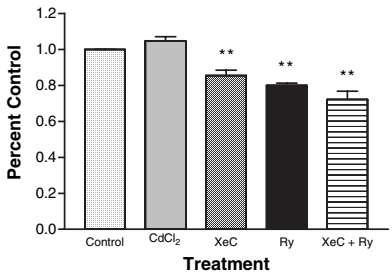

Fig. 6 Role of voltage-operated calcium channels and intracellular calcium stores in the epibatidine-evoked increase in intracellular calcium in mmα4β2 cells. Aequorin/coelenterizine-hcp-loaded mmα4β2 cells were stimulated with 1 μM epibatidine after 30 min incubation with vehicle (control), 100 μM $CdCl_2$, 30 μM ryanodine (Ry) and 10 μM xestospongin C (XeC) or 30 μM ryanodine + 10 μM xestospongin C (Ry + XeC). Immediately upon injection of epibatidine onto the cells, luminescence was recorded at 0.2 s intervals for 20 s. Data were calculated as the ratio of agonist-induced peak aequorin luminescence (L) divided by the sum of the possible aequorin luminescence (L_{max}; peak agonist induced luminescence + peak luminescence following cell lysis in the presence of 50 mM calcium). Results presented represent the percent L/L_{max} relative to the epibatidine response in the presence of vehicle. Data shown represent the mean ± SEM of between three and six independent aequorin transfections per drug treatment). Data were analyzed by means of one-way ANOVA. $^{**}p < 0.001$ relative to control response.

appear to be predominantly due to entry of calcium through the receptor channel with a contribution of ~ 28% from the release of calcium from intracellular stores.

Discussion

We report the functional characterization of a cell line that stably expresses a mouse α4β2 nAchR. This is the first report of a stable heterologous expression system for the characterization of mouse α4β2 nAchRs. Moreover, this is the first report where the aequorin-based luminescence assay was used to measure neuronal nAchR-mediated changes in intracellular calcium. The aequorin assay provides a new and relatively simple method to measure nAchR function in mammalian cell culture systems.

Consistent with previous reports (Buisson and Bertrand 2001; Nelson *et al*. 2003), stable expression of mouse α4β2 nAchRs in HEK293T cells leads to the expression of two receptor populations. The predominant subpopulation (90% of the whole-cell patch-clamp response) of receptors exhibits an EC_{50} value for Ach of 179 ± 22 μM and the minor component has an EC_{50} value for Ach of 3.36 ± 2.25 μM. Using HEK cells stably transfected with the human α4 and β2 nAchR subunits, Nelson *et al*. (2003) recently demonstrated that the receptor population with high Ach affinity (EC_{50} = 0.7 ± 0.4 μM) has a stoichiometry of $\alpha4_2\beta2_3$ and the low-affinity population (EC_{50} = 74 ± 6 μM) represents α4β2 nAchRs with a stoichiometry of $\alpha4_3\beta2_2$. Therefore, the low Ach sensitivity of the predominant α4β2 nAchR in the mmα4β2 cells is consistent with an α4β2 nAchR that has a stoichiometry of $\alpha4_3\beta2_2$.

Comparison of the aequorin assay-determined EC_{50} values for the mmα4β2 line with those of human α4β2 nAchRs stably expressed in HEK cells indicates that the pharmacology of the mouse and human α4β2 nAchR are very similar (Table 1). The correlation between the EC_{50} values for the mouse and human α4β2 cell lines for the four common agonists tested between studies (Ach, epibatidine, DMPP and nicotine) is 0.984 (r, $p < 0.01$, slope = 1.02) when compared with human α4β2-mediated changes in intracellular calcium (Chavez-Noriega *et al*. 2000) and 0.973 (r, $p < 0.05$, slope = 1.00) when compared with human α4β2-mediated $^{86}Rb^{+}$ efflux (Gopalakrishnan *et al*. 1996). Also, the mmα4β2 cell line exhibited an EC_{50} value for Ach activation (66.3 ± 2.28 μM) that is quite similar to the EC_{50} value for Ach observed in a variety of independently derived human α4β2 HEK stable cell lines (43.79 ± 1.18 μM, Gopalakrishnan *et al*. 1996; 100 μM, Chavez-Noriega *et al*. 2000; 74 ± 6 μM, Nelson *et al*. 2003) and to the EC_{50} value for Ach in oocytes when equal amounts of α4 and β2 cRNAs are injected (65.6 ± 20.2, Zwart and Vijverberg 1998).

When the pharmacology of the mmα4β2 cell line was compared with that of human α4β2 cells stably expressed in SH-EP cells (Eaton *et al*. 2003), no significant correlation

was detected (adjusted $R^2 = -0.18$, $p > 0.5$). This lack of correlation is driven by the ~ 35-fold lower EC_{50} values for Ach and epibatidine in the SH-EP cells. The observation that α4β2 nAchRs in SH-EP cells exhibit an EC_{50} value for Ach in the 1 μM range suggests that the receptor stoichiometry in this cell line may be $(\alpha4)_2(\beta2)_3$ (Zwart and Vijverberg 1998; Nelson *et al*. 2003; Zhou *et al*. 2003). However, there are other possible explanations for the differences in pharmacology of the α4β2 nAchRs expressed in the SH-EP cells relative to the HEK cells such as cell-type differences in lipid composition (Zanello *et al*. 1996) or cell-type specific receptor–protein interactions (Lin *et al*. 2002).

A $^{86}Rb^+$ efflux assay has been utilized to demonstrate that there are two major pharmacologically distinct responses in mouse brain synaptosomes that require the nAchR α4 and β2 subunits (Marks *et al*. 1999). The two α4- and β2-dependent components can be separated into a DHβE-sensitive and a DHβE-resistant component. A comparison of the pharmacological profile of the mmα4β2 cells with that of agonist-induced $^{86}Rb^+$ efflux from mouse brain synaptosomes indicates that the mmα4β2 cells exhibit an agonist pharmacology most similar to the DHβE-sensitive component (Fig. 7); the regression line for this comparison is essentially superimposed upon the line of identity ($r = 0.875$, slope = 1.00). In contrast, the regression line for the comparison between the EC_{50} values for the mmα4β2 cells and the DHβE-resistant response is distinct from the line of identity ($r = 0.94$, slope = 0.71). Agonist efficacies are also most similar between the mmα4β2 cells and the DHβE-sensitive response (Table 1). For example, TMA, an agonist that exhibits high efficacy for the DHβE-sensitive component but very poor efficacy for the DHβE-resistant component, displays high efficacy for the α4β2 nAchR expressed in the mmα4β2 cell line.

A comparison of antagonist inhibition profiles between the mmα4β2 cells and the mouse brain synaptosomal $^{86}Rb^+$ efflux DHβE-sensitive response demonstrated that the IC_{50} values for DHβE, DEC and MEC in the mmα4β2 cells are consistent with the IC_{50} values for these antagonists for the DHβE-sensitive component (Table 2, Fig. 7). In contrast, the mmα4β2 cells exhibited IC_{50} values for HEX and MLA that are 7–8-fold lower than the IC_{50} values for these antagonists for the DHβE-sensitive component of Rb^+ efflux. No attempt was made to compare the IC_{50} values from the mmα4β2 cell line with those of the DHβE-resistant component or the IC_{50}

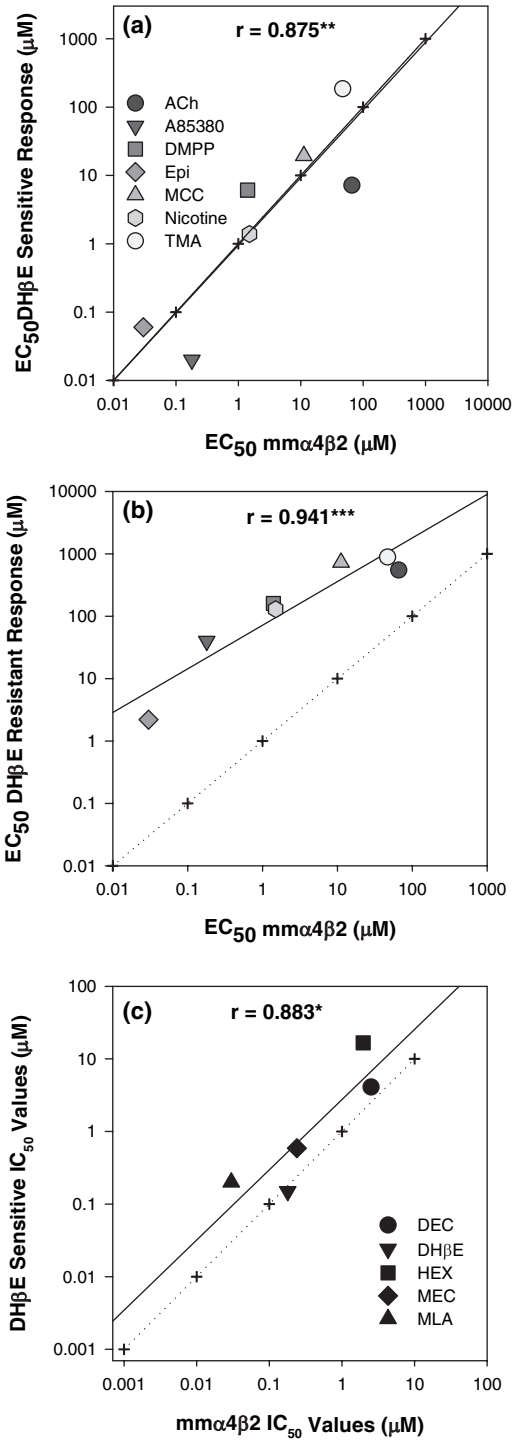

Fig. 7 Pharmacological comparison between mmα4β2 cells and nAchR-mediated $^{86}Rb^+$ efflux from mouse brain synaptosomes. (a) Comparison of agonist EC_{50} values between mmα4β2 cells and the DHβE-sensitive component of $^{86}Rb^+$ efflux from mouse brain synaptosomes. The solid line represents regression line for two nAchR-mediated responses. The dotted line with cross-hairs represents the line of identity. (b) Comparison of agonist EC_{50} values between mmα4β2 cells and the DHβE-resistant component of $^{86}Rb^+$ efflux from mouse brain synaptosomes. The solid line represents regression line for the two nAchR-mediated responses. The dotted line with cross-hairs represents the line of identity. (c) Comparison of antagonist IC_{50} values between mmα4β2 cells and the DHβE-sensitive component of $^{86}Rb^+$ efflux from mouse brain synaptosomes. The solid line represents regression line for the two nAchR-mediated responses. The dotted line with cross-hairs represents the line of identity. *$p < 0.05$; **$p < 0.01$; ***$p < 0.005$.

values of other stable lines because different agonists were used to evaluate the antagonists in the DHβE-resistant component and the other stable lines.

Owing to the similarities in their agonist pharmacologies and their similar sensitivity to the antagonist DHβE, it is tempting to speculate that the α4β2 nAchRs mediating nicotinic responses in the mmα4β2 cells possess the same stoichiometry and/or post-translational modifications as do the receptors that mediate the DHβE-sensitive component of $^{86}Rb^{+}$ efflux. However, the agonist and antagonist pharmacologies of the DHβE-sensitive component of $^{86}Rb^{+}$ efflux and the mmα4β2 cells are not identical. Consequently, despite the considerable similarities in pharmacology between the mmα4β2 cells and the DHβE-sensitive response, it is not clear whether a receptor with identical stoichiometry and/or post-translational modifications is responsible for both α4β2-mediated responses.

One potential explanation for the pharmacological differences between the mouse brain synaptosomes and mmα4β2 cells is the fact that the synaptosomes were prepared from a mouse strain that expresses an α4 subunit that has a threonine at amino acid position 529, whereas the mmα4β2 cell line expresses a receptor with an alanine at this position. Previous studies have shown that this polymorphism influences receptor function (Dobelis *et al*. 2002; Kim *et al*. 2003). The development of a cell line that expresses an α4β2 nAchR with the threonine variant of the α4 subunit would be useful to address this issue.

One striking difference in the pharmacology of the mmα4β2 cell line relative to the reported pharmacology of other α4β2 nAchRs is the very low IC_{50} value of the mmα4β2 cell line for MLA. The IC_{50} value of 31 ± 1.2 nM for MLA inhibition of receptor function in the mmα4β2 cells is not only lower than the IC_{50} value observed for this antagonist in inhibiting the DHβE-sensitive component of $^{86}Rb^{+}$ efflux (Marks *et al*. 1999), it also is considerably lower than the reported low micromolar IC_{50} values for MLA inhibition of other heterologous α4β2 nAchR expression systems (Buisson *et al*. 1996; Eaton *et al*. 2003). MLA has been shown to inhibit α7-containing nAchRs with IC_{50} values in the high picomolar to low nanomolar range (Alkondon *et al*. 1992; Palma *et al*. 1996; Virginio *et al*. 2002; Zhou *et al*. 2003). Owing to the substantial differences in reported IC50 values for MLA inhibition of α7 nAchRs versus other nAchR subtypes, MLA is generally regarded as a highly selective antagonist for nAchRs comprised of the α7 subunit. However, in addition to the data reported here, others have reported that MLA can inhibit non-α7-mediated responses in the low nanomolar range. Clarke and Reuben (1996) demonstrated that nicotine-stimulated [^{3}H]-dopamine release from rat brain striatal synaptosomes can be inhibited by MLA with an IC_{50} value of 38 nM. Similarly, Grady *et al*. (1997) found that the transient phase of nicotine-stimulated dopamine release from mouse brain synaptosomes was inhibited by MLA with an IC_{50} value of 36 nM. Receptors containing the α7 subunit are not likely involved in [^{3}H]-dopamine release from either mouse or rat brain synaptosomes as the classic α7 antagonist α-bungarotoxin does not inhibit nicotinic agonist-stimulated [^{3}H]-dopamine release from either species (Rapier *et al*. 1990; Grady *et al*. 1992) and nicotinic agonist-stimulated [^{3}H]-dopamine release does not differ between α7 subunit null mutant mice and their wild-type controls (Salminen *et al*. 2004). In contrast, Grady *et al*. (2002) have demonstrated that the β2 subunit is an absolute requirement for nicotine-induced [^{3}H]-dopamine release and the α4 subunit is essential for ~ 80% of nicotine-stimulated [^{3}H]-dopamine release (Salminen *et al*. 2004). Furthermore, Mogg *et al*. (2002) have shown that a presumed α3/α6β2β2 nAchR in rat striatum is inhibited by low nanomolar concentrations of MLA. These data indicate that MLA can inhibit non-α7-mediated responses at low nanomolar concentrations in heterologous expression systems as well as in rodent brain synaptosomes and suggest that this antagonist may not be as selective in the low nanomolar range for α7-containing nAchRs as previously thought.

The inhibition of non-α7-mediated responses by low nanomolar concentrations of MLA was observed in neurotransmitter release and intracellular calcium-based assays. In contrast, the reported inhibition of α4β2 nAchRs by high nanomolar to low micromolar concentrations of MLA were determined by ion flux (Marks *et al*. 1999; Eaton *et al*. 2003) and electrophysiological (Buisson *et al*. 1996) assays. Therefore, the potency of MLA at inhibiting nAchR-mediated responses may be dependent upon the assay used to evaluate the drug. In support of this possibility, we have determined the IC_{50} value for MLA inhibition of mmα4β2 receptor function using whole-cell patch-clamp electrophysiology. Using this method, we observed an IC_{50} value for MLA of 0.43 ± 1.2 μM (data not shown). This IC_{50} value for MLA is more consistent with the IC_{50} values previously reported for MLA inhibition of α4β2 nAchRs when measured by $^{86}Rb^{+}$ efflux or electrophysiological methods (Buisson *et al*. 1996; Marks *et al*. 1999; Eaton *et al*. 2003).

Fitch *et al*. (2003) also found significant differences in the pharmacology of an α3β4 cell line when evaluated by different methods. This group observed that the nicotinic antagonist mecamylamine was equipotent at inhibiting receptor function in an intracellular calcium assay and an $^{86}Rb^{+}$ efflux assay but ~ 25-fold less potent at inhibiting responses in the membrane potential assay. The agonist A85380 also was ~ 6-fold less potent at stimulating responses in the intracellular calcium assay compared with the $^{86}Rb^{+}$ efflux assay and 30 times less potent when compared with the membrane potential assay. Other substantial differences in agonist pharmacologies across methodologies were also reported by Fitch *et al*. (2003). Unfortunately, MLA was not evaluated in this study. Similarly, in the mmα4β2 cells, considerable differences

in the potencies of Ach (EC_{50}, aequorin: 66.3 ± 2.2 μM; whole-cell recording: 179 ± 22 μM), TMA (EC_{50}, aequorin: 46.9 ± 0.36 μM; whole cell recording: 243 ± 1.1 μM; data not shown) and MLA (IC_{50}, aequorin: 0.03 ± 0.0012 μM; whole-cell recording: 0.43 ± 1.2 μM) were observed when determined by aequorin and electrophysiological methods. Ach, TMA and MLA were the only compounds tested in the mmα4β2 cells by both methods. Regardless, these data and the data reported by Fitch *et al.* suggest that caution should be used when assigning the nAchR subtype specificity of a nicotinic compound based on the potency of the compound as determined by a single method of functional analysis.

The data reported here also established that the α4β2 nAchR-mediated increase in intracellular calcium in the mmα4β2 cells is due predominantly to direct entry of calcium through the receptor channel. Release of calcium from both ryanodine- and IP_3-sensitive intracellular stores also appears to contribute to the increase in intracellular calcium. Dantroline, another inhibitor of ryanodine-sensitive calcium release, inhibited epibatidine-evoked changes in intracellular calcium to the same extent as ryanodine (data not shown) indicating that the effect of ryanodine on intracellular calcium release was not due to a non-specific effect of the drug. However, it cannot be entirely ruled out that the apparent blockade of IP_3-sensitive calcium stores by xestospongin C is due to a non-specific effect of the drug such as blockade of the nAchR channel or other ion channel (Ozaki *et al*. 2002). There was no detectable contribution of high-voltage-sensitive calcium channels to the rise in intracellular calcium. However, HEK293T cells likely do not possess the full complement of voltage-sensitive calcium channels present in neurons. Therefore, these results must be interpreted with caution. Regardless, these data suggest that α4β2 nAchRs do not require the contribution of high-voltage-sensitive calcium channels in order to elicit a discernable rise in intracellular calcium. The lack of requirement for voltage-sensitive calcium channels for α4β2-mediated changes in intracellular calcium is consistent with other reports on heterologously expressed α4β2 nAchRs (Chavez-Noriega *et al*. 2000; Michelmore *et al*. 2002) and α4β2 nAchRs measured *in situ* (Nayak *et al*. 2001).

Previous studies have shown that the mechanism of nAchR-mediated changes in intracellular calcium levels is subtype specific (Gray *et al*. 1996; Tsuneki *et al*. 2000; Shoop *et al*. 2001; Dajas-Bailador *et al*. 2002). For example, several groups have reported that α7 subunit-containing nAchRs do not require the contribution of voltage-sensitive calcium channels in order to elicit agonist-induced changes in intracellular calcium (Gray *et al*. 1996; Tsuneki *et al*. 2000; Shoop *et al*. 2001; Dajas-Bailador *et al*. 2002). In contrast, changes in intracellular calcium resulting from the stimulation of some nAchRs that contain the α3 subunit (Shoop *et al*. 2001; Dajas-Bailador *et al*. 2002) and some nAchRs that contain the β2 subunit (Tsuneki *et al*. 2000) appear to require the activation of voltage-sensitive calcium channels. This suggests that the effect of nAchR activation on calcium-dependent cellular processes depends upon which particular subtype or subtypes are activated. Therefore, nicotinic agonist effects on such calcium-dependent cellular processes as signal transduction pathways, transcription factor expression and activation, synaptic plasticity and neuroprotection would depend upon which nAchR subtype is activated. Further studies to evaluate nAchR subtype-specific changes in intracellular calcium and the affected downstream signaling pathways should provide a better appreciation for the role of specific nAchR subtypes in brain function and disease.

Acknowledgements

The authors would like to thank Mr Brody Flanagin and Mr Paul Jenkins for their expert technical assistance. This work supported by DA-14369 from the National Institutes of Health (NIDA).

References

Alkondon M., Pereira E. F., Wonnacott S. and Albuquerque E. X. (1992) Blockade of nicotinic currents in hippocampal neurons defines methyllycaconitine as a potent and specific receptor antagonist. *Mol. Pharmacol.* **41**, 802–808.

Alkondon M., Pereira E. F. and Albuquerque E. X. (1996) Mapping the location of functional nicotinic and gamma-aminobutyric acid A receptors on hippocampal neurons. *J. Pharmacol. Exp. Ther.* **279**, 1491–1506.

Benwell M. E., Balfour D. J. and Anderson J. M. (1988) Evidence that tobacco smoking increases the density of (–)-[^{3}H]nicotine binding sites in human brain. *J. Neurochem.* **50**, 1243–1247.

Berridge M. J. (1998) Neuronal calcium signaling. *Neuron* **21**, 13–26.

Bertrand D., Galzi J. L., Devillers-Thiery A., Bertrand S. and Changeux J. P. (1993) Mutations at two distinct sites within the channel domain M2 alter calcium permeability of neuronal alpha 7 nicotinic receptor. *Proc. Natl Acad. Sci. USA* **90**, 6971–6975.

Breese C. R., Marks M. J., Logel J., Adams C. E., Sullivan B., Collins A. C. and Leonard S. (1997) Effect of smoking history on [^{3}H]nicotine binding in human postmortem brain. *J. Pharmacol. Exp. Ther.* **282**, 7–13.

Brini M., Marsault R., Bastianutto C., Alvarez J., Pozzan T. and Rizzuto R. (1995) Transfected aequorin in the measurement of cytosolic Ca^{2+} concentration ([Ca^{2+}]c). A critical evaluation. *J. Biol. Chem.* **270**, 9896–9903.

Buisson B. and Bertrand D. (2001) Chronic exposure to nicotine upregulates the human (alpha)4(beta)2 nicotinic acetylcholine receptor function. *J. Neurosci.* **21**, 1819–1829.

Buisson B., Gopalakrishnan M., Arneric S. P., Sullivan J. P. and Bertrand D. (1996) Human alpha4beta2 neuronal nicotinic acetylcholine receptor in HEK 293 cells: A patch-clamp study. *J. Neurosci.* **16**, 7880–7891.

Butt C. M., King N. M., Stitzel J. A. and Collins A. C. (2004) Interaction of the nicotinic cholinergic system with ethanol withdrawal. *J. Pharmacol. Exp. Ther.* **308**, 591–599.

Castro N. G. and Albuquerque E. X. (1995) Alpha-bungarotoxin-sensitive hippocampal nicotinic receptor channel has a high calcium permeability. *Biophys. J.* **68**, 516–524.

Champtiaux N., Han Z. Y., Bessis A., Rossi F. M., Zoli M., Marubio L., McIntosh J. M. and Changeux J. P. (2002) Distribution and pharmacology of alpha 6-containing nicotinic acetylcholine receptors analyzed with mutant mice. *J. Neurosci.* **22**, 1208–1217.

Chavez-Noriega L. E., Gillespie A., Stauderman K. A. *et al.* (2000) Characterization of the recombinant human neuronal nicotinic acetylcholine receptors alpha3beta2 and alpha4beta2 stably expressed in HEK293 cells. *Neuropharmacology* **39**, 2543–2560.

Clarke P. B. and Reuben M. (1996) Release of [^{3}H]-noradrenaline from rat hippocampal synaptosomes by nicotine: mediation by different nicotinic receptor subtypes from striatal [^{3}H]-dopamine release. *Br. J. Pharmacol.* **117**, 595–606.

Dajas-Bailador F. A., Mogg A. J. and Wonnacott S. (2002) Intracellular Ca^{2+} signals evoked by stimulation of nicotinic acetylcholine receptors in SH-SY5Y cells: contribution of voltage-operated Ca^{2+} channels and Ca^{2+} stores. *J. Neurochem.* **81**, 606–614.

Dobelis P., Marks M. J., Whiteaker P., Balogh S. A., Collins A. C. and Stitzel J. A. (2002) A polymorphism in the mouse neuronal alpha4 nicotinic receptor subunit results in an alteration in receptor function. *Mol. Pharmacol.* **62**, 334–342.

Eaton J. B., Peng J. H., Schroeder K. M., George A. A., Fryer J. D., Krishnan C., Buhlman L., Kuo Y. P., Steinlein O. and Lukas R. J. (2003) Characterization of human alpha4beta2-nicotinic acetylcholine receptors stably and heterologously expressed in native nicotinic receptor-null SH-EP1 human epithelial cells. *Mol. Pharmacol.* **64**, 1283–1294.

Epping-Jordan M. P., Picciotto M. R., Changeux J. P. and Pich E. M. (1999) Assessment of nicotinic acetylcholine receptor subunit contributions to nicotine self-administration in mutant mice. *Psychopharmacology (Berl.)* **147**, 25–26.

Fitch R. W., Xiao Y., Kellar K. J. and Daly J. W. (2003) Membrane potential fluorescence: a rapid and highly sensitive assay for nicotinic receptor channel function. *Proc. Natl Acad. Sci. USA* **100**, 4909–4914.

Flynn D. D. and Mash D. C. (1986) Characterization of L-[^{3}H]nicotine binding in human cerebral cortex: comparison between Alzheimer's disease and the normal. *J. Neurochem.* **47**, 1948–1954.

Gafni J., Munsch J. A., Lam T. H., Catlin M. C., Costa L. G., Molinski T. F. and Pessah I. N. (1997) Xestospongins: potent membrane permeable blockers of the inositol 1,4,5-trisphosphate receptor. *Neuron* **19**, 723–733.

Gopalakrishnan M., Monteggia L. M., Anderson D. J., Molinari E. J., Piattoni-Kaplan M., Donnelly-Roberts D., Arneric S. P. and Sullivan J. P. (1996) Stable expression, pharmacologic properties and regulation of the human neuronal nicotinic acetylcholine alpha4beta2 receptor. *J. Pharmacol. Exp. Ther.* **276**, 289–297.

Grady S., Marks M. J., Wonnacott S. and Collins A. C. (1992) Characterization of nicotinic receptor-mediated [^{3}H]dopamine release from synaptosomes prepared from mouse striatum. *J. Neurochem.* **59**, 848–856.

Grady S. R., Grun E. U., Marks M. J. and Collins A. C. (1997) Pharmacological comparison of transient and persistent [^{3}H]dopamine release from mouse striatal synaptosomes and response to chronic L-nicotine treatment. *J. Pharmacol. Exp. Ther.* **282**, 32–43.

Gray R., Rajan A. S., Radcliffe K. A., Yakehiro M. and Dani J. A. (1996) Hippocampal synaptic transmission enhanced by low concentrations of nicotine. *Nature* **383**, 713–716.

Gueorguiev V. D., Zeman R. J., Meyer E. M. and Sabban E. L. (2000) Involvement of alpha7 nicotinic acetylcholine receptors in activation of tyrosine hydroxylase and dopamine beta-hydroxylase gene expression in PC12 cells. *J. Neurochem.* **75**, 1997–2005.

Kim H., Flanagin B. A., Qin C., Macdonald R. L. and Stitzel J. A. (2003) The mouse *Chrna4* A529T polymorphism alters the ratio of high to low affinity alpha4beta2 nAChRs. *Neuropharmacology* **45**, 345–354.

Klink R., de Kerchove D. A., Zoli M. and Changeux J. P. (2001) Molecular and physiological diversity of nicotinic acetylcholine receptors in the midbrain dopaminergic nuclei. *J. Neurosci.* **21**, 1452–1463.

Lin L., Jeanclos E. M., Treuil M., Braunewell K. H., Gundelfinger E. D. and Anand R. (2002) The calcium sensor protein visinin-like protein-1 modulates the surface expression and agonist sensitivity of the alpha4beta2 nicotinic acetylcholine receptor. *J. Biol. Chem.* **277**, 41 872–41 878.

Lindstrom J. M. (2003) Nicotinic acetylcholine receptors of muscles and nerves: comparison of their structures, functional roles, and vulnerability to pathology. *Ann. NY Acad. Sci.* **998**, 41–52.

Lowry O. H., Rosebrough N. H., Farr A. C. and Randall R. T. (1951) Protein measurement with the Folin phenol reagent. *J. Biol. Chem.* **193**, 265–275.

Lu Y., Grady S., Marks M. J., Picciotto M., Changeux J. P. and Collins A. C. (1998) Pharmacological characterization of nicotinic receptor-stimulated GABA release from mouse brain synaptosomes. *J. Pharmacol. Exp. Ther.* **287**, 648–657.

Marks M. J., Burch J. B. and Collins A. C. (1983) Effects of chronic nicotine infusion on tolerance development and nicotinic receptors. *J. Pharmacol. Exp. Ther.* **226**, 817–825.

Marks M. J., Smith K. W. and Collins A. C. (1998) Differential agonist inhibition identifies multiple epibatidine binding sites in mouse brain. *J. Pharmacol. Exp. Ther.* **285**, 377–386.

Marks M. J., Whiteaker P., Calcaterra J., Stitzel J. A., Bullock A. E., Grady S. R., Picciotto M. R., Changeux J. P. and Collins A. C. (1999) Two pharmacologically distinct components of nicotinic receptor-mediated rubidium efflux in mouse brain require the beta2 subunit. *J. Pharmacol. Exp. Ther.* **289**, 1090–1103.

Michelmore S., Croskery K., Nozulak J., Hoyer D., Longato R., Weber A., Bouhelal R. and Feuerbach D. (2002) Study of the calcium dynamics of the human alpha4beta2, alpha3beta4 and alpha1beta1gammadelta nicotinic acetylcholine receptors. *Naunyn Schmiedebergs Arch. Pharmacol.* **366**, 235–245.

Mogg A. J., Whiteaker P., McIntosh J. M., Marks M., Collins A. C. and Wonnacott S. (2002) Methyllycaconitine is a potent antagonist of alpha-conotoxin-MII-sensitive presynaptic nicotinic acetylcholine receptors in rat striatum. *J. Pharmacol. Exp. Ther.* **302**, 197–204.

Nayak S. V., Dougherty J. J., McIntosh J. M. and Nichols R. A. (2001) Ca(2+) changes induced by different presynaptic nicotinic receptors in separate populations of individual striatal nerve terminals. *J. Neurochem.* **76**, 1860–1870.

Nelson M. E., Kuryatov A., Choi C. H., Zhou Y. and Lindstrom J. (2003) Alternate stoichiometries of alpha4beta2 nicotinic acetylcholine receptors. *Mol. Pharmacol.* **63**, 332–341.

Nordberg A. and Winblad B. (1986) Reduced number of [^{3}H]nicotine and [^{3}H]acetylcholine binding sites in the frontal cortex of Alzheimer brains. *Neurosci. Lett.* **72**, 115–119.

Owens J. C., Balogh S. A., McClure-Begley T. D., Butt C. M., Labarca C., Lester H. A., Picciotto M. R., Wehner J. M. and Collins A. C. (2003) Alpha4beta2* nicotinic acetylcholine receptors modulate the effects of ethanol and nicotine on the acoustic startle response. *Alcohol Clin. Exp. Res.* **27**, 1867–1875.

Ozaki H., Hori M., Kim Y. S., Kwon S. C., Ahn D. S., Nakazawa H., Kobayashi M. and Karaki H. (2002) Inhibitory mechanism of xestospongin-C on contraction and ion channels in the intestinal smooth muscle. *Br. J. Pharmacol.* **137**, 1207–1212.

Pacheco M. A., Pastoor T. E., Lukas R. J. and Wecker L. (2001) Characterization of human alpha4beta2 neuronal nicotinic receptors stably expressed in SH-EP1 cells. *Neurochem. Res.* **26**, 683–693.

Palma E., Bertrand S., Binzoni T. and Bertrand D. (1996) Neuronal nicotinic alpha 7 receptor expressed in *Xenopus* oocytes presents five putative binding sites for methyllycaconitine. *J. Physiol.* **491**, 151–161.

Picciotto M. R., Zoli M., Lena C., Bessis A., Lallemand Y., LeNovere N., Vincent P., Pich E. M., Brulet P. and Changeux J. P. (1995) Abnormal avoidance learning in mice lacking functional high-affinity nicotine receptor in the brain. *Nature* **374**, 65–67.

Ragozzino D., Barabino B., Fucile S. and Eusebi F. (1998) Ca^{2+} permeability of mouse and chick nicotinic acetylcholine receptors expressed in transiently transfected human cells. *J. Physiol.* **507**, 749–757.

Rapier C., Lunt G. G. and Wonnacott S. (1990) Nicotinic modulation of [^{3}H]dopamine release from striatal synaptosomes: pharmacological characterisation. *J. Neurochem.* **54**, 937–945.

Role L. W. and Berg D. K. (1996) Nicotinic receptors in the development and modulation of CNS synapses. *Neuron* **16**, 1077–1085.

Ryan R. E., Ross S. A., Drago J. and Loiacono R. E. (2001) Dose-related neuroprotective effects of chronic nicotine in 6-hydroxydopamine treated rats, and loss of neuroprotection in alpha4 nicotinic receptor subunit knockout mice. *Br. J. Pharmacol.* **132**, 1650–1656.

Salminen O. S., Murphy K. L., McIntosh J. M., Drago J., Marks M. J., Collins A. C. and Grady S. R. (2004) Subunit composition and pharmacology of two classes of striatal presynaptic nicotinic acetylcholine receptors mediating dopamine release in mice. *Mol. Pharmacol.* **65**, 1526–1535.

Seguela P., Wadiche J., Dineley-Miller K., Dani J. A. and Patrick J. W. (1993) Molecular cloning, functional properties, and distribution of rat brain alpha 7: a nicotinic cation channel highly permeable to calcium. *J. Neurosci.* **13**, 596–604.

Shafaee N., Houng M., Truong A., Viseshakul N., Figl A., Sandhu S., Forsayeth J. R., Dwoskin L. P., Crooks P. A. and Cohen B. N. (1999) Pharmacological similarities between native brain and heterologously expressed alpha4beta2 nicotinic receptors. *Br. J. Pharmacol.* **128**, 1291–1299.

Sharma G. and Vijayaraghavan S. (2001) Nicotinic cholinergic signaling in hippocampal astrocytes involves calcium-induced calcium release from intracellular stores. *Proc. Natl Acad. Sci. USA* **98**, 4148–4153.

Shoop R. D., Chang K. T., Ellisman M. H. and Berg D. K. (2001) Synaptically driven calcium transients via nicotinic receptors on somatic spines. *J. Neurosci.* **21**, 771–781.

Steinlein O. K. (2004) Nicotinic receptor mutations in human epilepsy. *Prog. Brain Res.* **145**, 275–285.

Stitzel J. A., Jimenez M., Marks M. J., Tritto T. and Collins A. C. (2000) Potential role of the alpha4 and alpha6 nicotinic receptor subunits in regulating nicotine-induced seizures. *J. Pharmacol. Exp. Ther.* **293**, 67–74.

Stitzel J. A., Dobelis P., Jimenez M. and Collins A. C. (2001) Long sleep and short sleep mice differ in nicotine-stimulated $^{86}Rb^{+}$ efflux and alpha4 nicotinic receptor subunit cDNA sequence. *Pharmacogenetics* **11**, 331–339.

Tritto T., Stitzel J. A., Marks M. J., Romm E. and Collins A. C. (2002) Variability in response to nicotine in the LSxSS RI strains: potential role of polymorphisms in alpha4 and alpha6 nicotinic receptor genes. *Pharmacogenetics* **12**, 197–208.

Truong A., Xing X., Forsayeth J. R., Dwoskin L. P., Crooks P. A. and Cohen B. N. (2001) Pharmacological differences between immunoisolated native brain and heterologously expressed rat alpha4beta2 nicotinic receptors. *Brain Res. Mol. Brain Res.* **96**, 68–76.

Tsuneki H., Klink R., Lena C., Korn H. and Changeux J. P. (2000) Calcium mobilization elicited by two types of nicotinic acetylcholine receptors in mouse substantia nigra pars compacta. *Eur. J. Neurosci.* **12**, 2475–2485.

Ungrin M. D., Singh L. M., Stocco R., Sas D. E. and Abramovitz M. (1999) An automated aequorin luminescence-based functional calcium assay for G-protein-coupled receptors. *Anal. Biochem.* **272**, 34–42.

Vernino S., Amador M., Luetje C. W., Patrick J. and Dani J. A. (1992) Calcium modulation and high calcium permeability of neuronal nicotinic acetylcholine receptors. *Neuron* **8**, 127–134.

Vernon W. I. and Printen J. A. (2002) Assay for intracellular calcium using a codon-optimized aequorin. *Biotechniques* **33**, 730–734.

Virginio C., Giacometti A., Aldegher L., Rimland J. M. and Terstappen G. C. (2002) Pharmacological properties of rat alpha 7 nicotinic receptors expressed in native and recombinant cell systems. *Eur. J. Pharmacol.* **445**, 153–161.

Whitehouse P. J., Martino A. M., Antuono P. G., Lowenstein P. R., Coyle J. T., Price D. L. and Kellar K. J. (1986) Nicotinic acetylcholine binding sites in Alzheimer's disease. *Brain Res.* **371**, 146–151.

Whiting P. J. and Lindstrom J. M. (1988) Characterization of bovine and human neuronal nicotinic acetylcholine receptors using monoclonal antibodies. *J. Neurosci.* **8**, 3395–3404.

Xiao Y., Meyer E. L., Thompson J. M., Surin A., Wroblewski J. and Kellar K. J. (1998) Rat alpha3/beta4 subtype of neuronal nicotinic acetylcholine receptor stably expressed in a transfected cell line: pharmacology of ligand binding and function. *Mol. Pharmacol.* **54**, 322–333.

Zanello L. P., Aztiria E., Antollini S. and Barrantes F. J. (1996) Nicotinic acetylcholine receptor channels are influenced by the physical state of their membrane environment. *Biophys. J.* **70**, 2155–2164.

Zhou Y., Nelson M. E., Kuryatov A., Choi C., Cooper J. and Lindstrom J. (2003) Human alpha4beta2 acetylcholine receptors formed from linked subunits. *J. Neurosci.* **23**, 9004–9015.

Zhu P. J. and Chiappinelli V. A. (1999) Nicotine modulates evoked GABAergic transmission in the brain. *J. Neurophysiol.* **82**, 3041–3045.

Zoli M., Moretti M., Zanardi A., McIntosh J. M., Clementi F. and Gotti C. (2002) Identification of the nicotinic receptor subtypes expressed on dopaminergic terminals in the rat striatum. *J. Neurosci.* **22**, 8785–8789.

Zwart R. and Vijverberg H. P. (1998) Four pharmacologically distinct subtypes of alpha4beta2 nicotinic acetylcholine receptor expressed in *Xenopus laevis* oocytes. *Mol. Pharmacol.* **54**, 1124–1131.